REPORT DOCUMENTATION PAGE

AFRL-SR-BL-TR-02-

0733

1. AGENCY USE ONLY *(Leave blank)*	2. REPORT DATE	3. REPO
	03/19/2002	FINAL (11/01/1997 TO 05/31/2001

4. TITLE AND SUBTITLE
FATIGUE AND FRACTURE CHARACTERIZATION OF AIRCRAFT ALUMINUM ALLOYS DAMAGED BY PRIOR CORROSION

5. FUNDING NUMBERS
F49620-98-1-0050

6. AUTHOR(S)
DR. J.D. BALDWIN

7. PERFORMING ORGANIZATION NAME(S) AND ADDRESS(ES)
UNIVERSITY OF OKLAHOMA
THE SCHOOL OF AEROSPACE AND MECHANICAL ENGINEERING
865 ASP AVENUE, ROOM FH 212
NORMAN, OK 73109-1052

8. PERFORMING ORGANIZATION REPORT NUMBER

9. SPONSORING/MONITORING AGENCY NAME(S) AND ADDRESS(ES)
AFOSR
801 N. RANDLOPH STREET
ARLINGTON, VA 22202

20020417 266

11. SUPPLEMENTARY NOTES

12a. DISTRIBUTION AVAILABILITY STATEMENT

Approved for public release;
distribution unlimited.

12b. DISTRIBUTION CODE

13. ABSTRACT *(Maximum 200 words)*

At the time of the initiation of this project, there was no comprehensive data describing corrosion's effect on the fatigue and fracture behavior of aluminum alloys typically found in aging aircraft. One of the primary objectives of this project was to perform experimental and analytic characterizations of these materials response for three aluminum alloys (2024-T3, 7075-T6 and 7178-T6, all widely used in order aircraft) in the presence of prior corrosion. Because the typical aircraft's operation cycle leads to the supposition that corrosion and fatigue are series events (as opposed to simultaneous corrosion and fatigue), we made experimental test specimens that had artificially-grown corrosion damage in them. The aim was to develop the necessary material response data to be used in structural integrity inspection interval determinations. Specifically, fatigue crack growth rates and fracture toughness data were developed. For each alloy, the experimental variables were material condition (ranging from no corrosion through several degrees of damage), stress ratio and relative humidity in the air environment. Here, we quantified corrosion damage as the percent of material lost, based on the nominal specimen thickness. A multiple replication factorial experimental design provided the data and analysis of variance techniques were used to address the hypotheses that the experimental variables affect the crack growth rates and that any observed differences can be accounted for by considering only the thickness reduction caused by corrosion. For each alloy, crack growth rate relationships (e.g., da/dN versus AK) were developed that account for corrosion damage. The fracture characterization focused on the plane stress fracture toughness values (Kc) for varying levels of corrosion damage and varying specimen

14. SUBJECT TERMS

15. NUMBER OF PAGES

16. PRICE CODE

17. SECURITY CLASSIFICATION OF REPORT	18. SECURITY CLASSIFICATION OF THIS PAGE	19. SECURITY CLASSIFICATION OF ABSTRACT	20. LIMITATION OF ABSTRACT
UNCLASSIFIED	UNCLASSIFED	UNCLASSIFIED	

Final Report

Fatigue and Fracture Characterization of Aircraft Aluminum Alloys Damaged by Prior Corrosion

Air Force Office of Scientific Research Contract No. F49620-98-1-0050

Submitted by
J.D. Baldwin, Ph.D., P.E.
Associate Professor
School of Aerospace & Mechanical Engineering
University of Oklahoma
865 Asp Avenue, Room 212
Norman, Oklahoma 73072

March 19, 2002

The School of Aerospace and Mechanical Engineering

865 Asp Avenue, Room FH 212
Norman, Oklahoma 73019-1052

THE UNIVERSITY OF OKLAHOMA

Final Report

Fatigue and Fracture Characterization of Aircraft Aluminum Alloys Damaged by Prior Corrosion

Air Force Office of Scientific Research Contract No. F49620-98-1-0050

Submitted by
J.D. Baldwin, Ph.D., P.E.
Associate Professor
School of Aerospace & Mechanical Engineering
University of Oklahoma
865 Asp Avenue, Room 212
Norman, Oklahoma 73072

March 19, 2002

Abstract

At the time of the initiation of this project, there was no comprehensive data describing corrosion's effect on the fatigue and fracture behavior of aluminum alloys typically found in aging aircraft. One of the primary objective of this project was to perform experimental and analytical characterizations of these material responses for three aluminum alloys (2024-T3, 7075-T6 and 7178-T6, all widely used in older aircraft) in the presence of prior corrosion. Because the typical aircraft's operation cycle leads to the supposition that corrosion and fatigue are series events (as opposed to simultaneous corrosion and fatigue), we made experimental test specimens that had artificially-grown corrosion damage in them. The aim was to develop the necessary material response data to be used in structural integrity inspection interval determinations. Specifically, fatigue crack growth rates and fracture toughness data were developed. For each alloy, the experimental variables were material condition (ranging from no corrosion through several degrees of damage), stress ratio and relative humidity in the air environment. Here, we quantified corrosion damage as the percent of material lost, based on the nominal specimen thickness. A multiple replication factorial experimental design provided the data and analysis of variance techniques were used to address the hypotheses that the experimental variables affect the crack growth rates and that any observed differences can be accounted for by considering only the thickness reduction caused by corrosion. For each alloy, crack growth rate relationships (e.g., da/dN versus ΔK) were developed that account for corrosion damage. The fracture characterization focused on the plane stress fracture toughness values (K_C) for varying levels of corrosion damage and varying specimen thicknesses. A set of critical fracture toughness values for each sheet thickness and level of corrosion damage were developed. The material behavior relationships to be developed here, da/dN vs. ΔK and K_C that account for corrosion damage, are now available for incorporation into structural integrity inspection intervals, thus allowing more rational account to be taken of corrosion's effect on airframe durability.

Acknowledgments

This research was funded in part by the U.S. Air Force Oklahoma City Air Logistics Center and by the Air Force Office of Scientific Research under contract No. F49620-98-1-0050.

Thanks are due to Mr. Don Nieser, from the Oklahoma City Air Logistics Center for providing the KC-135 parts that became the fatigue test specimens, and also to Messrs. Bob Rennell, Geoff Mitchell, and Bart Gardner of ARINC for helping to provide these parts. Mr. Billy Mays and Mr. Greg Williams also contributed their time and effort in obtaining these parts and in helping turn these into specimens, and their effort is greatly appreciated.

This research benefitted enormously from the time my student, Mr. David Denman, spent at the Air Force Research Laboratory at Wright-Patterson Air Force Base. I want to thank Dr. Tom Mills for his guidance during the early stages of this effort and also to Mr. Clare Paul and Dr. Scott Fawaz for their input and assistance. Thanks are also due to Mr. Jim Harter at Wright-Patterson Air Force Base.

Others who provided insight and guidance include Dr. Robert Piascik and Dr. James Newman, both at NASA-Langley, Dr. Wayne Whaley of Oklahoma Christian University/ARINC, and Mr. Joe Luzar, of Boeing-Wichita who was a great source of historical information on aluminum material characterization.

Table of Contents

List of Figures

List of Tables

Nomenclature

Symbol		Description
a	=	Crack length
A_c	=	Corroded area
A_t	=	Total area
B	=	Thickness of specimen
C	=	Material parameter
da/dN	=	Crack growth rate per cycle of applied stress
k	=	Curve fit parameter
K	=	Stress intensity factor
K_c	=	Fracture toughness
m	=	Material parameter
N	=	Number of cycles
P	=	Load
R	=	Stress ratio
TL	=	Thickness loss
v	=	Crack opening displacement
W	=	Width of specimen
W_a	=	Specimen's weight after corrosion
W_b	=	Specimen's weight before corrosion
σ	=	Normal stress
μ	=	Distribution mean

Subscript		Description
bl	=	Baseline
cor	=	Corroded
max	=	Maximum
min	=	Minimum

1.0: Introduction

It is now well known that corrosion is a common occurrence in the USAF fleet, particularly in the older systems such as the C/KC-135, and because of its widespread occurrence throughout the fleet, corrosion has become a technical *and* an economic issue. The primary goal of this project was to experimentally explore the fatigue and fracture behavior of three common aircraft aluminum alloys (2024-T3, 7075-T6 and 7178-T6) in the presence of prior corrosion damage. Because of lack of material availability from the Oklahoma City Air Logistics Center, we did not conduct any material characterization on the 7178-T6 material. The data gathered here is now available to be used for multiple site damage (MSD) analysis of structures with assumed levels of corrosion damage. In such a damaged structure, failing to account for corrosion's effects on material properties will result in inspection intervals that are too long given current USAF damage tolerance guidelines. The results of this project have expanded the capabilities of the USAF Corrosion Fatigue Program in three ways:

1) A corrosion damage benchmark study was conducted where the ASTM EXCO solution was used to attack sample coupons. By exposing coupons to the solution for varying times, we developed a relationship between depth of corrosion attack and time of exposure for each material studied. The depth of attack was quantified by 1) measuring the weight loss of the specimen due to corrosion, 2) direct measurement by a point micrometer, and 3) sectioning a coupon in the corroded region and imaging the section through a video capture system working through an optical microscope. Such a relationship will streamline the process of producing fatigue crack growth and fracture toughness specimens with predetermined levels of damage.

2) Unlike most other investigations into the fatigue crack growth behavior of corrosion-damaged aluminum alloys, where only one level of corrosion damage was studied, we developed an experimental design that had the level of corrosion damage as an experimental variable. ASTM E 647 fatigue crack growth rate testing provided da/dN vs. ΔK data for the two alloys. Experimental treatments will be level of corrosion damage (measured as percent of specimen

thickness lost), stress ratio and relative humidity. Three specimens will be used for each experimental treatment value; a total of 48 specimens were used in this task. In this way, we addressed the question of how much corrosion damage is required to significantly affect the fatigue cracking behavior. Also, we addressed the very important issue of whether the increased crack growth rates observed in corrosion-damaged metal can be adequately described by a reduced effective thickness of the crack zone. Regression and analysis of variance methods provided the statistical basis for our conclusions regarding observed crack growth rates.

3) For the first time, we have investigated fracture toughness degradation in the presence of different levels of corrosion damage. This is a critical issue, because there is currently no data available on this adverse effect. The fracture toughness is the factor that determines the critical crack length at the onset of unstable fracture; experience has shown that prior corrosion will tend to reduce the fracture toughness and shorten the critical crack length. Using the ASTM E 561 procedures as a guide, we will again use level of corrosion attack as an experimental variable, testing specimens having several levels of damage.

1.1: Research Problem

It is now well-known that the average ages of commercial and military aircraft fleets are increasing, prompting an intense examination of the trade-offs between economic efficiency and airworthiness. As the fleets age, corrosion damage and its impact on airframe durability become of particular concern. As Schutz noted [1995], fatigue strength and corrosion parameters combine in a synergistic manner that has not yet been completely described. The technical challenges facing operators of aging aircraft came into sharp focus in April 1988 when Aloha Airlines Flight 243 experienced a catastrophic failure of the forward fuselage. Although the cause of the Aloha structural failure was formally given as multiple site damage, there was certainly a component of corrosion damage involved. Corrosion-induced aircraft accidents have occurred throughout the history of aviation. Campbell and Lahey [1984] reported that, since

1927, there had been over 60 accidents worldwide at least partly attributable to corrosion damage. In a more recent study, Hoeppner, et al. [1995] update Campbell's statistics, reporting that since 1975 there have been nearly 700 domestic incidents and accidents in which corrosion was at least a contributing factor. Hendricks [1991] estimated the cost of a major commercial aircraft overhaul at $2-20 million dollars. Compared with the approximately $50-100 million required for a new aircraft, the economic incentive for operating older planes is apparent. For operators of large fleets, however, the economic burden of keeping aging aircraft operational is becoming prohibitive. In 1994, a U.S. Air Force study showed that the maintenance costs of repairing corrosion damage alone had reached the $1-3 billion per year level [Chang, 1995]. Since the Aloha accident, the issues involved in operating aging aircraft fleets have received increased attention from agencies such as the U.S. Air Force, U.S. Navy, National Aeronautics and Space Administration and Federal Aviation Administration. The major thrust of the investigation undertaken here was to address the effect of corrosion on the fatigue and fracture performance of structural aluminum alloys commonly found in older aircraft with particular emphasis on corrosion's effect on required inspection intervals.

The U.S. Air Force's fleet of nearly 700 C/KC-135 tanker aircraft, first designed in the mid-1950's, now has an average age of over 30 years with none newer than 24 years old [Chang, 1995]. By virtue of its vintage, the C/KC-135 was designed before the damage tolerant design philosophy was mandated for all USAF aircraft and therefore, does not include features such as crack arrestors commonly found in more recent designs. Corrosion of the aluminum fuselage panels and wing skins has been observed with increasing regularity, particularly in lap joints and around fastener holes. In fact, corrosion has proven to be an insidious enemy, often found only after disassembly of the structure, despite the use of nondestructive inspection systems. These tendencies are observed not only in the C/KC-135 fleet, but in other aging weapons systems as well. Because of the prohibitive cost to replace the fleet, these aircraft are considered a national asset and, as such, will be expected to serve well into the next century [Lincoln, 1995]. In fact,

it is anticipated that the C/KC-135's will be one of the last of the current USAF transport platforms to be retired. Because there is no plan to replace these aircraft in the near future, the effect of corrosion on structural integrity must be quantified and incorporated into the fleet maintenance procedures.

Like many large military aircraft, the C/KC-135 fleet spends most of its time on the ground exposed to a spectrum of atmospheric contaminants that promote corrosion of the structure. During the ground time, the airframe is essentially unloaded. On the other hand, fully loaded conditions occur during the relatively short periods when the aircraft are in flight (and in a relatively unaggressive environment at altitude). Because of this loading characteristic, it may be assumed that the loading cycles occur such that fatigue cracks will nucleate and grow, in a relatively unaggressive environment, in metal that has already experienced corrosion and a corrosive environment. Unlike the typical corrosion fatigue process, where corrosion and fatigue occur simultaneously, the processes appear to be largely (but certainly not completely) uncoupled for aging aircraft.

Figure 1-1 shows schematically the relationship between crack length and time for a fatigue-critical structural element. Initially, all cracks are assumed to be of length a_0, the largest undetectable flaw size. The a versus N behavior illustrated is a complicated function of crack and structure geometry (ΔK), load history, and material response (da/dN vs. ΔK), where the actual curve must be established for each structural detail of interest. The critical crack length, a_c, represents the longest crack that can be sustained before unstable fracture occurs at time N_1, an event controlled by the material's fracture toughness, K_C. An inspection interval is defined for a structural element by taking one half of the time required to grow a crack of critical length and requiring inspection at that time. This inspection is therefore based on the time to grow a crack of length a_i; time $\frac{1}{2}N_1$ in the Figure represents this inspection point for baseline, noncorroded material.

Figure 1-1 shows that there are two ways in which corrosion damage affects the

inspection interval. First, the presence of corrosion damage is now known to be responsible for accelerated crack growth. This effect is represented by the a versus N curve labeled "prior corrosion." At all times, a crack growing in corrosion-damaged material will be longer than one growing in noncorroded material, all else equal. Time $½N_2$ corresponds to the inspection time that would be required solely on the basis of accelerated crack growth. The second effect is the reduction in fracture toughness, as depicted by the lower, "prior corrosion," line a_c. The combined effects of accelerated crack growth and reduced fracture toughness are reflected in the inspection interval time $½N_3$. Clearly if we account for both cracking and residual strength changes, the required inspection time will be shorter than if we account for each separately, or if we ignore the corrosion damage altogether. Thus, failing to account for corrosion damage can cause nonconservative assumptions to be made about the required inspection interval. At the present time, there is insufficient fatigue crack growth rate (da/dN vs. ΔK) and fracture toughness (K_C) data to make a good estimate of the shortened inspection interval required for airframe details damaged by corrosion. The goal of this project was to create a body of material response data that begins to address this issue.

1.2: Literature Survey

Essentially all of the published work in corrosion fatigue has focused on the behavior of new (i.e., noncorroded) materials in various corrosive environments [Gangloff, 1990; Kemp, et al., 1993; Gangloff, et al., 1994]. Although the existing literature provides valuable insight into the corrosion fatigue behavior of metals, it fails to address the metal's response to loading after corrosion has already occurred. Investigations into the fatigue cracking performance of aluminum alloys damaged by prior corrosion have appeared only recently, largely in response to the Aloha accident. Leybold et al., [1958] studied the effects of atmospheric corrosion on aluminum fatigue by exposing 2024-T3 and 7075-T6 specimens to the coastal environment at Langley Field, Virginia, while subjecting them to reversed bending fatigue where they were

tested until fracture. Leybold concluded that the fatigue life of these materials was reduced by factors ranging from essentially zero up to about three. In 1961, Harmsworth [1961] systematically studied the total fatigue life (i.e., rotating beam *S-N* curve behavior) of aluminum alloy 2024-T3 damaged by prior corrosion in a NaCl solution and concluded that increasing surface roughness was an indicator of reduced fatigue life. Person [1975] used three NaCl solutions to induce pitting corrosion in 2014, 5083 and 7075 alloys exposed for up to 400 hours. The specimens were subjected to constant amplitude, reversed bending loading and reduction of the fatigue strength of up to about 50 percent was observed. More recently, Chaudhuri, et al., [1994] and Du, et al. [1995] performed similar total life, stress-based characterizations using NaCl solutions; Mills and Hoeppner [1995] carried out *S-N* testing using specimens corroded in the ASTM EXCO solution [ASTM G 34]. In all cases, a reduction in the fatigue life was observed. Although Chaudhuri reported no quantitative evaluation of the corrosion damage, Du used a profilometer to measure surface roughness. Mills qualitatively classified corrosion damage as "light" through "very severe" corresponding to between 7 and 48 hours of exposure to the corrosive solution. It should be emphasized that each of these studies addressed the total fatigue life of the test specimens, not the fatigue crack growth rate. As a result, the forgoing results might be of importance in addressing the effect of prior corrosion on crack nucleation, but are of little use in the context of the fracture mechanics-based USAF damage tolerant design philosophy.

Only recently have fracture mechanics-based experiments designed to quantify the fatigue response of corroded metal begun to appear. Chubb, et al. [1991a, 1991b, 1995] examined the effect of exfoliation corrosion on the fatigue crack growth rates of 2024-T351 and 7178-T6 alloys exposed to the EXCO solution for 96 hours. Chubb's data indicates that at low ΔK levels, the corroded material experienced crack accelerations of up to five times over noncorroded material. Scheuring and Grandt [1994, 1995] used 2024-T3, 7075-T6 and 7178-T6 materials taken from retired C/KC-135 aircraft corroded in service. The corrosion damage was

qualitatively described as "light" and "moderate" and the resulting specimen thickness was further estimated by optical microscopy. Scheuring notes that the lightly corroded material shows little difference in crack growth behavior compared to noncorroded material. Their data also shows that the acceleration in crack growth tends to diminish as the stress ratio R increases. Scheuring also raises the interesting possibility that the observed higher crack growth rates may be caused by other factors in addition to corrosion-induced thinning. After accounting for the actual specimen thickness, cracks appeared to continue to grow faster than in baseline material, suggesting that perhaps another process was at work in the crack zone. While these two research teams report valuable results, the conclusions drawn are based on qualitative comparison of the results. Lacking a statistical analysis, it is difficult to separate the effects of the test parameters such as corrosion damage level, stress ratio and test environment.

The C/KC-135 Corrosion Fatigue test program [Luzar, 1995] was designed by Boeing to collect fatigue crack growth rate data for pre-corroded materials and compare it with data for baseline, noncorroded samples of the same materials (2024-T3, 2024-T4, 7075-T6 and 7178-T6). This program was based on a 2^3 factorial experimental design with treatments being material condition (as-received vs. artificially-corroded), stress ratio ($R = 0.05$ versus $R = 0.50$) and relative humidity (<15% R.H. air versus >85% R.H. air). Four laboratories were involved in the round robin testing. No attempt was made to create corroded specimen population with differing degrees of corrosion damage, however, the corrosion damage was to be "severe." The test specimens were taken from retired C/KC-135 fuselage and wing skins. When compared with the baseline (BL) data, the data show accelerated crack growth rates and exhibit the expected stress ratio (R) behavior, i.e., higher mean stresses cause faster crack growth.

In an attempt to draw valid conclusions about the observed increase in crack growth rates, statistical analyses of 7075-T6 da/dN vs. ΔK data have been performed [Baldwin, 1996]. In that analysis, the experimental treatments were material condition (as-received, artificially corroded), stress ratio ($R = 0.05$, $R = 0.50$) and humidity (<15% RH, >85% RH). The goal was

to use the statistical analysis to determine whether the apparent change in crack growth rate behavior was due to random variability or if it was due to the treatments. Without offering any experimental or statistical proof, Doerfler, et al. [1993] proposed that any increase in crack growth rate could be explained solely on the basis of the reduction in thickness due to corrosion. The statistical analysis suggested in this case that the differences in material condition were a significant factor in the observed differences in crack growth rate. The data sets were limited, however, by the relatively few data points from each specimen, by intra-laboratory variations in testing results and by the presence of only one level of corrosion damage. The additional crack growth rate testing proposed here is designed to fill in the gaps in the existing data base on these metals and settle this issue conclusively.

While the available crack growth rate data is very limited in scope, the effect of prior corrosion on fracture toughness is essentially unexplored. Chubb, et al. [1995] provide the only fracture toughness data currently available in the literature for precorroded aluminum. Using seven 2.5 mm thick 7178-T6 sheet exposed to up to 192 hours in an EXCO solution, Chubb found an 11 percent reduction in fracture toughness after 96 hours exposure. There was no quantification of the corrosion damage beyond giving the time of specimen exposure to the EXCO solution. While Chubb's data supports the assumption that K_C is reduced in the presence of corrosion damage, it is insufficient given that it addresses only one sheet thickness for one alloy.

In the wake of the Aloha accident, a growing body of research has appeared addressing the implications of multi-site damage in the loss of structural integrity in fuselage structures. Computational methods, such as finite elements [Beuth and Hutchinson, 1994; Tong, et al., 1994] and boundary elements [Blackburn, et al., 1995] have been implemented to study various aspects of the MSD problem, including fastener loading effects [Tong, 1994] and crack linkup phenomena [Jeong and Brewer, 1995]. Experimental studies of the behavior of groups of collinear cracks have also been reported by Broek [1993], Molent and Jones [1993] and

Samavedam and Hoadley [1994]. It should be noted that all these studies were concerned with "local" effects active near the cracks. On a more global scale, two groups have also made contributions toward the analysis of large sections of fuselage with embedded cracks. A technique known as the elastic-plastic finite element alternating method (EPFEAM) has been used to analyze fuselage sectors several frames wide with cracks near or through frames [Atluri and Tong, 1991; Park, et al., 1992; Singh, et al., 1994; Pyo, et al., 1995]. In a similar fashion, Lockheed's *STAGS* program has evolved to the point where it can be used to analyze full fuselage rings [Rankin, et al., 1993]. Using hierarchical modeling techniques (i.e., a "global-local" analysis), the *FRANC3D* fracture analysis code can now be driven by *STAGS* allowing the behavior of a fuselage crack to be based on the loads carried by the entire ring section [Harris, et al., 1995]. None of these studies, however, have included the effect of corrosion damage in the material response parameters.

1.3: Research Goals

When the fatigue crack growth and fracture toughness data are analyzed, they will permit us to address the significance of corrosion damage from the perspective of airframe inspection intervals. The data developed in this project will provide information about the material-controlled aspects of the inspection interval and will be applicable to many fuselage and wing skin details. As mentioned above, the existing data relating corrosion damage with fatigue and fracture behavior is incomplete with respect to damage quantification, degrees of damage and alloy diversity. Up to this point, all of the conclusions in the literature regarding corrosion's effect on crack growth are based on qualitative evaluations of the data. Only through statistical analysis can we begin to have confidence in such conclusions.

2.0: Corrosion Fatigue Crack Growth [vu99]

2.0.1: Background

Scheuring and Grandt [1994, 1995] obtained materials harvested from aging aircraft with some degree of corrosion damage quantified by the thickness loss, weight loss, and also by visual inspection. Then tests were conducted to assess the effect of prior corrosion damage on the monotonic stress-strain response, cyclic stress-life response, and crack growth behavior. Within the context of the present research, we were primarily interested in the crack growth results.

Scheuring's crack growth analyses were conducted using aluminum alloys 7075-T6, 2024-T3, and 7178-T8 with stress ratios $\left(R = \sigma_{\min} / \sigma_{\max}\right)$ of 0.5 and 0.1. The results were compared between the corroded and baseline samples of the same material and stress ratio. The data for the corroded material showed a small increase in the crack growth rate for 7075-T6, but no significant change in 2024-T6 and in 7178-T6.

The USAF "Round Robin Testing" program [Luzar, 1995] was designed to provide fatigue crack growth data for artificially corroded and baseline C/KC-135 aircraft fuselage and upper wing skin materials. The materials were divided into two groups: artificially corroded and non-corroded (baseline). One half of the specimens from each of the four different materials (aluminum alloys 2024-T3, 2024-T4, 7075-T6 and 7178-T6) was corroded, and the remaining material was used as the baseline specimen set. Testing was conducted at two levels of humidity (Dry < 15% RH and Wet > 85% RH), at two stress ratios ($R = 0.05$ and $R = 0.50$), and at two cyclic frequencies (0.1 Hz and 10 Hz).

By observing the crack growth rate versus stress intensity range in log-log coordinates, it was found that the fatigue crack growth data for the baseline and artificially corroded materials indicated some differences. However, these differences apparently become insignificant when compared to Boeing historical data. In addition, these data, which were not corrected for net

section area loss, largely fall within the upper band of the historic baseline data scatter. It was also concluded that no frequency effect was observed between 0.1Hz and 10Hz cycling.

Baldwin, et al., [1997] did an analysis of the Round Robin data to address the observed differences in baseline and corroded material behavior from a statistical point of view. The corroded specimens were thinner thus causing a higher net section stress and accelerated crack growth rate compared with the baseline specimens. To correct for this effect, the crack growth rate data were adjusted for corroded net section area. Note that these specimens indicated a material loss ranging between 12% to 16%, and an average of 15% thickness loss was used for comparison. The apparent corrosion differences were only observed in the uncorrected 7075-T6 data which was resolved by adjusting for 15% corroded net section thickness loss.

Furthermore, Baldwin, et al, [1997] did a statistical analysis, which provided another way to compare the crack growth behavior of corrosion damaged material with the original baseline material. While the Round Robin data was initially compared by observation the plots of the baseline and artificially corroded material data to the historic data, this research used a statistical analysis to compare the two or more fatigue crack growth rate (FCGR) experiments. In the case of the Round Robin 7075-T6 data, a statistically significant difference was found between the FCGR behavior of baseline and artificially corroded materials. The implementation of this analysis will be reviewed later in this section.

2.0.2: Objective

Through all of the previous research, the corrosion damage level of the test specimens, aged 7075-T6, was relatively small (~15% thickness loss) as compared with observed real levels of corrosion in aging aircraft, and there is not enough information to answer some important questions: "Is there a different crack growth rate in corroded materials at different levels of corrosion versus non-corroded (i.e., baseline) materials?"; "If so, is that difference the result of thickness loss or due to another factor?"; and "If the thickness loss is corrected, will the

difference go away?" In addition, new 7075-T6 aluminum, which would be used in modern aircraft, has not been studied yet.

From Baldwin, et al. [1997], we know that only in aluminum alloy 7075-T6 was there a significant difference observed in the crack propagation data between the corroded and baseline cases. Alloy 2024-T3 showed very minor differences in crack growth rates between the baseline and corroded conditions, therefore the 2024 series alloys were not included in this effort. Crack growth rate studies were conducted on 7075-T6 materials from two sources: material cut from a retired USAF KC-135, and new 7075-T6. The study of the aged 7075-T6 highlights the effects of corrosion on aging aircraft, which may help to maintain the current aging aircraft to prevent failure due to corrosion, while the study of new 7075-T6 will point out any differences attributable to improved processing. In addition, the Round Robin testing achieved only an approximate 15% thickness loss; here we extended the corrosion level to 30% thickness loss.

2.1: Corrosion Studies and Specimen Preparation

Our goal was to induce a 25% to 30% thickness loss in the test specimens by immersion in the ASTM G-34 [ASTM G 34] EXCO solution. The corrosion procedure involved immersing the specimens in the EXCO solution consisting of 234 grams of NaCl (Crystal, Reagent A.C.S), 50 grams of KNO_3 (Crystal, Reagent A.C.S), and 6.3 milliliters HNO_3-70% (Reagent A.C.S) in one liter of distilled water. The EXCO solution should have an apparent initial pH of 0.4. The pH of the EXCO solution was measured by an electronic pH meter (Corning 307 series) with $\pm$ 0.01 accuracy. The standard recommends that the solution be made in sufficient quantity to give a liquid volume to metal surface area ratio of 10 to 30 mL/cm^2 (65 to 200 mL/in^2).

Because we had no guide for determining the time of immersion to achieve the target thickness loss, a trial test was conducted to study the time-damage relationship. The trial test specimens consisted of three inch by four inch chips of the two materials to be used in later

fatigue experiments. A chip was covered on one side by 3M electroplating tape (Scotch Brand, Core Series 2-0300) to protect that side from corrosion. It was then weighed and dipped into the EXCO solution. Every day, the chip was taken out of the EXCO solution and weighed on an Ainsworth PC300 scale (300 ± 0.01 grams), and on that basis a calculation of the weight loss was made. ASTM G-34 requires that the EXCO solution pH should not rise higher than about 3.0 during the corrosion period. We found that the pH typically exceeded 3.0 after about two days due to the lost concentration of the solution. Therefore, the solution was replaced with a fresh one after 48 hours to insure high corrosion efficiency. In this case, four solution changes were required to achieve the required 30% thickness loss. On this basis, the corrosion protocol for the fatigue specimens called for 192 hours of immersion in EXCO solution with changes every 48 hours.

2.1.1: Test Specimen Fabrication

The crack growth test specimens were designed according to ASTM E-647 [ASTM E 647] for the middle tension M(T) configuration (Figure 2.1) fabricated both from the aged KC-135 material and from the new 7075-T6 aluminum alloy sheet. The specimen nominal thickness was 0.063 inches for the new material, and 0.084 inches for the aged material. Due to limitations of the aged material source (e.g., stiffener placement, rivet consistency, etc.), 3.0 inch wide specimens were used for that material.

The corrosion damaged specimen group was corroded in the EXCO solution. The specimens were wrapped in the 3M electroplating tape to minimize corrosion of the non-test area leaving only a one inch wide strip across the test specimen to be corroded (Figure 2.1). To achieve the required 30% thickness reduction, the specimens were immersed for a total of 192 hours, and were then rinsed to clean off all chemicals. Once the tape was unwrapped, the specimen was sent out for fabrication of the Electrical Discharge Machine (EDM) notch (Figure 2.2) in accordance with the requirement of the ASTM E647 standard.

2.1.2: Corrosion Level Validation

It was very hard to make *a priori* predictions of the degree of corrosion damage in the material, because the corrosion processes are not easy to predict and control. In addition, the corroded surfaces are not smooth with some places corroded more deeply than others, thus making the direct observation more difficult. However, there are two related ways of making estimates of the corrosion level in the specimens: the indirect percentage weight loss and the direct measurement of the percentage thickness loss. The weight loss method is based on the weight of specimen before and after corrosion, and the direct measurement method is based on the average of random measurements of the thickness of the corroded area.

The measured weight loss was converted to a percentage thickness loss as follows. The specimens were weighed before and after corrosion by the Ainsworth PC300 scale and the weight difference was calculated. Also the ratio of specimen area exposed to corrosion to the total specimen area was calculated. The percentage thickness loss was calculated from the relationship

$$\%TL = \frac{(W_b - W_a)}{\left(A_c / A_t\right) * W_b} * 100 \qquad (2.1)$$

where W_b and W_a are the weights of specimen before and after corrosion, and A_c and A_t are the corrosion area and total area on one side of the specimen, respectively.

The direct estimate of thickness loss was based on two measurement techniques: direct measurement using a point micrometer and measurement through a microscope image. The direct point micrometer measurements (Starrett Model 760) were taken randomly at ten different places in the corroded area before the fatigue test. The microscope image measurement (Olympus Model B30 at 5X magnification) used an image of the crack surface of the specimen after fatigue testing, and also was measured randomly at ten different places in the microscope image. The average percentage thickness loss was calculated using the expression

$$\%TL = \frac{B - \left(\frac{1}{10}\right)\sum_{i}^{10} B_{ci}}{B} * 100 \qquad (2.2)$$

where B_{ci} is the thickness of the corroded area of each measurement, and B is the initial (nominal) thickness of the specimen.

The percentage of thickness loss of each fatigue specimen was calculated by the weight loss method and the direct measurement method, which shown in Table 2-1 for the aged material and Table 2-2 for new material. Also, a random sampling of several specimens was made from the microscope image, also shown in Tables 2-1 and 2-2. These tables show that the relative level of corrosion given by the two different methods differs by less than 8%, a difference that is considered insignificant. In addition, direct measurement of the microscope images confirmed the prior results. Therefore, the results are considered very acceptable, and we can confirm that the 30% thickness loss due to corrosion was achieved.

2.2: Experimental Procedures

The experimental testing was conducted under constant amplitude loading on both groups of the artificially corroded and baseline material. The test was also conducted using two different environmental conditions (dry: < 15% RH, and wet: > 85% RH), and two different stress ratios ($R = 0.05$ and $R = 0.50$).

2.2.1: Environmental Control

All of the crack growth rate tests were conducted at room temperature. Each group of corrosion and baseline specimens was divided into two environmental conditions, a dry environment defined as being less than 15% relative humidity, and a wet environment defined as being non-condensing with greater than 85% relative humidity. Humidity data was measured at the environmental testing chamber (Figure 2-3), using a humidity meter (EXTech Model

444712 Hygro-Thermometer). Low humidity vapor was created by the passing the air through a desiccant-filled tower; high humidity vapor was provided by bubbling air through a column of reagent-grade laboratory water.

2.2.2: Crack Growth Rate Testing

For the crack growth testing, the applied load profile was a constant amplitude sine wave. In addition to the specimen condition and environment, an additional experimental treatment, the stress ratio, was varied. Two values of R ($= \sigma_{min} / \sigma_{max}$) were used, $R = 0.05$ and $R = 0.50$. Combining the two different stress ratios and the two relative humidity conditions gives four test blocks for each of the corroded material and baseline material groups. The tests were conducted for both aged material and new material as shown in Table 2-3.

The test was conducted on the 20-kip MTS machine using digital computer control. Pre-cracking and crack growth rate testing were conducted in accordance with ASTM E-647. The applied load range was set to suit the required stress ratio and to achieve a crack tip stress intensity of 7.0 ksi$\sqrt{in}$ at the end of pre-cracking. After the pre-cracking process, the crack length was measured at both ends of the crack by reading indirectly through the meter with a Gaertner 30X traveling microscope at intervals consistent with the requirements of the Standard.

2.2.3: Crack Growth Results

The following graphs (Figures 2-4 through 2-7) show how the fatigue cracks growth rate of the aged and new 7075-T6 material changes due to the effects of 30% thickness loss. From the Figures it is apparent that the fatigue crack growth rate for the corroded material is shifted up and to the left, meaning that the FCGR's will be faster than the baseline material for either of the applied environmental conditions. After correction for thickness loss, the FCGR's for both groups of experimental data appear to lie on top each other. The statistical analysis of this data will be presented in the next section.

Figure 2-4 shows the FCGR *da/dN* vs. ΔK for the stress ratio $R = 0.05$ and relative humidity greater than 85% ; this data has not been corrected for thickness loss. The thickness loss correction is accomplished by using a stress value based on the 30% thickness loss in the ΔK calculation; the nominal stress based on the nominal thickness and applied load does not change. Figure 2-5 shows that correcting the data for thickness loss reduces the difference between the two data groups. These findings are consistent through all combinations of stress ratio and relative humidity for the aged 7075-T6 material.

In Figures 2-6 and 2-7 similar FCGR results are observed for the 30% corrosion damage in the new material. Observing Figure 2-6, the data for the corroded group and baseline group show significant differences. Again, after correcting for thickness loss, those differences appear less significant or not significant at all, as shown in Figure 2-7; this result is also consistent across all combinations of stress ratio and relative humidity applied to these specimens.

As expected, the results for 30% corrosion of both aged and new materials are similar to the 15% corroded specimens of the Round Robin Test [Luzer, 1995; Baldwin, 1995]. However, the FCGR *da/dN* of the corrosion specimen grew much faster than the baseline specimens and even faster than the 15% corroded specimens. Therefore, a thickness loss up to 30% makes the FCGR *da/dN* vs. ΔK data move farther to the left and up, which increases the difference between the corroded and baseline specimens. Similar to the 15% corrosion data, the difference between both groups was reduced to insignificance, when the correct thickness was taken into the calculation. Full data for the FCGR experiments is available in [Vu, 1999].

2.3: Statistical Analysis of Crack Growth Data

Because the graphs presented in the previous section do not quantify differences in behavior between the baseline materials and corroded materials, the following statistical analysis was developed to answer the question "Are the observed differences in the *da/dN* vs. ΔK data from replicated experiments with different experimental treatments statistically significant?".

The statistical analysis was made by using the *da/dN* vs. ΔK data divided into two groups: artificially corroded and baseline. Then, a curve fit curve was made through the FCGR data for each specimen. A 4th order polynomial curve was used to fit the data. From each of these curve fits, the value of *da/dN* at any value of ΔK of interest for each experiment was calculated, then the mean value of each of the two groups was computed. Finally, the null hypothesis t-test was used that compared the equality of the mean *da/dN* for each of the two groups [Baldwin, et al., 1997].

2.3.1: Analysis

The fatigue crack growth rate data described in this research is typically modeled using the Paris' equation, which has shown that fatigue crack growth experimental data can be consolidated by plotting the crack velocity (*da/dN*) against the stress intensity range (ΔK). This approach has been successfully applied to crack propagation fatigue analysis, and the log-log *da/dN* vs. ΔK plot has become the standard way of presenting the experimental fatigue crack growth data. Paris' equation, Equation 2.3, reflects the experimental observation that when plotted on log-log coordinates, fatigue crack growth data typically has a region that is approximately on a straight line. The Paris equation is [Paris, et al., 1961]

$$\frac{da}{dN} = C\Delta K^m \tag{2.3}$$

where C and m are material specific parameters.

The analysis begins by fitting a curve through each set of FCGR data. These curve fits allow interpolation between data points to estimate *da/dN* at any convenient value of ΔK, rather

$$\log\frac{da}{dN} = k_0 + k_1(\log\Delta K) + k_2(\log\Delta K)^2 + k_3(\log\Delta K)^3 + k_4(\log\Delta K)^4 \tag{2.4}$$

that at the actual values that normally do not coincide for every experimental data set. In this

analysis, a simple fourth order polynomial model was used to make the curve fit and is given by

Previous research has introduced many models, but this equation has a shape that is very representative of the experimental FCGR data. In addition, it has the computational advantage of being a linear regression calculation, as compared with the problematic nonlinear regression of other models. It is important to note that this curve fit is not being recommended as a general description of FCGR data, but only for this current statistical analysis. This model indicated a reasonable reflection of the data, at least in the interval where the experiment data exists, with coefficients of determination of these curve fits typically in the 0.94 to 0.98 range.

After all of the curve fits were available for each group of specimen data, then calculation of the crack growth rates could be done at any value of ΔK of interest in the data range. For this research, ΔK = 9, 10, 11, 12, 13, 14, 15, 16 and 17 ksi$\sqrt{}$inch were used to estimate the crack growth rate for each of set data. From the curve fit expressions, the collection of data representing the value of *da/dN* was computed at the given value of ΔK for both experimental populations of interest (i.e., corroded, baseline). Thus, for this analysis the experimental treatment to be considered was the material condition.

To compare the effects of the experimental treatment on crack growth rate, a statistical hypothesis test has been formulated to deal with this problem. The Student t-test examines the

$$H_0: \quad \mu_{BL} = \mu_{COR} \qquad (2.5)$$

null hypothesis that the mean of the baseline sample (μ_{BL}) at a given value of ΔK is equal to the mean of the corroded sample, (μ_{COR})

If the t-test results indicated that the test failed to reject the null hypothesis, the conclusion was that there were no effects of the experimental treatment. Otherwise, we could conclude that the experiment treatment had caused a difference in crack growth rate. In this analysis, the t-test was conducted at the 0.05 significance level.

2.3.2: Results of Statistical Analysis

The statistical analysis used the SigmaStat software to calculate the curve fits through all the data sets. Ten, the coefficients of these curves were entered back in to SigmaStat to calculate the crack growth rate at each of the convenient stress intensity factor values for the comparison. Each of the data sets was then run through a series of statistical tests: the Normality test, the Equal Variance test, and the t-test with 95% confidence.

The results of statistical analysis are given in Table 2-4 for the 30% corroded specimens. It shows that the significant difference will go away if the thickness loss was accounted for in the analysis. Exceptions occurred, where the data was failed either by the Normal test, the Equal Variance test, or both, in which cases no analysis was made. There are 3 cases noted by the sign (*) where human error in reading the crack length may have influenced the results or where the thickness loss of the specimens was larger than the average was used in correction.

Also, because data for some environmental conditions and stress ratio cases are so few (data lost to the yield stress and plastic zone size conditions), there is not enough data to do the statistical analysis at same values of ΔK. Therefore, Table 2-4 only shows the incomplete statistical analyses. However, this problem would be eliminated by using a wider specimen, which give more data for analysis.

2.4: Concluding Remarks - Fatigue Crack Growth

This effort focused on a study of the effect of prior corrosion on fatigue crack growth rate in 7075-T6 aluminum alloys. It was hoped that this study would provide a better understanding of the impact of corrosion on fatigue crack propagation in aged and new materials.

The corrosion protocol gave a simple way to determine the damage level of corroded material. By combination of two different methods, the weight method and the direct measurement method, we have more confidence on the results of the percentage corrosion. In additional, the direct measurement on microscope images confirm the results, therefore the

assertion of 30% thickness loss due to corrosion was supported. The result of 30% thickness loss was achieved by immersing specimens in the ASTM EXCO solution for 192 hours.

By observing the experimental test data, we can conclude that corrosion damage affected the fatigue crack growth rate, primarily because the thickness of the material was reduced due to the corrosion process. If the thickness loss was corrected for the FCGR of the two groups appear lie on top of each other. The statistical analysis confirmed that the observation of thickness reduction being responsible for accelerated FCGR, and gives a more confidence in the conclusion.

By combining the results of this research and the Round Robin Testing [Luzar, 1995; Baldwin, 1995; Baldwin et al., 1997] research, the conclusion for the impact of prior corrosion on crack propagation are as follows:

- The crack growth rate shows a significant difference between the artificially corroded material at any level of corrosion and the baseline groups of aged 7075-T6 materials and new 7075-T6 materials.

- The FCGR increase in corroded material that was caused by increasing the stress of the net section area due to the thickness loss. This finding is consistent across the stress ratio and relative humidity ranges used here.

- Different material (new and aged) and different level of corrosion (15% and 30%) show similar results, if the corrected thickness take into calculation.

3.0: Corrosion Impact on Residual Strength

The objective of this component of the study was to analyze the slow-stable crack growth in plane stress, middle tension M(T) specimens under increasing axial loads and to determine experimentally the Mode-I plane stress fracture toughness R-curves for representative aircraft aluminum alloys. The study also explored the relation between the fracture strength for corroded panels by comparing with baseline, non-corroded specimens. The experimental program for fracture strength of aluminum covered alloys 2024-T3 (0.040 and 0.063 inch thickness) and 7075-T6 (0.063 and 0.090 inch thickness). Specimens used in the experiments were in the middle tension M(T) configuration measuring 4 inches wide and 12 inches long (c.f., Figure 2-1).

This section details the preparation of artificially corroded specimens using the ASTM EXCO standard ASTM G-34. All the specimens were saw cut in the center using a jewelers saw and were pre-cracked to facilitate slow crack growth during the subsequent monotonic tensile testing. A clip-gage was attached to the specimen at the center of the crack growth axis for measuring the crack opening displacement (COD). All of the loading and data acquisition was controlled using MTS Teststar II software. The crack length was also recorded using an optical microscope on a traveling stage.

The data collected from the computer and user readings were processed as specified in ASTM Standards E 561-81 to obtain the crack growth resistance curve (R-curve). The R-curve obtained was found to be independent of the initial crack length of the specimen. The crack growth resistance value at the onset of the unstable crack growth is regarded as the fracture strength of the specimen and the values are listed in the result section. The analysis of data for the corroded panels shows that the R-curve depends on the thickness of the specimen and that thickness loss due to corrosion results in changes in the fracture toughness of the materials under consideration.

3.0.1: Previous Efforts

The fracture toughness can be defined as the resistance to fracture from applied load conditions on a given material having a pre-existing crack. The fracture toughness of a material is experimentally found by conducting monotonic tensile load testing on an appropriate test machine.

Initially, research was carried out to determine the fracture toughness in specimens thick enough to demonstrate plane strain behavior. Linear Elastic Fracture Mechanics (LEFM) concepts were used in the calculations since the plastic-zone developed is small and can be expressed as a function of stress-intensity factor, K. These efforts established a single fracture toughness value K_{IC}, the plane strain fracture toughness.

Aerospace industries are predominantly occupied with sheet metal applications that require plane stress analysis. ASTM Committee E-24 on Fracture Testing of High Strength Materials was involved in determining the fracture strength of high strength sheet materials. Early research efforts were attempted with a belief that a single K_C value exists which defines the instability criteria for fracture, however, the K_C value was found to rise and fall with the increase in width and attain a constant minimum value at a certain minimum width. Hence subsequent researchers carried out experiments that included testing of very wide specimens, up to 48 inches wide.

The R-curve concept, introduced in 1954, suggested against the existence of a single value of K_C for all types and sizes of specimens. The concept used an energy approach and stated "that the strain energy release rate and the fracturing work rate must be equal at onset of instability, and that they are unlikely to differ widely in magnitude as fracturing continues" (in reference to a central crack in a flat plate). Also Irwin and Kies [1954], the authors of the above concept, suggested decreasing fracture resistance with crack extension which stabilizes later to a constant value.

In 1959, Irwin [1959] modified his earlier R-curve concept with a rising crack growth

resistance with relative crack extension. The rise in resistance with crack growth is attributed to the fact that the plastic-zone size grows with the crack extension. Krafft, et al. [1961] compiled several investigations on aluminum alloy 7075-T6, and presented a paper that depicts R-curve plotted with absolute crack extension, Δa, rather than relative crack extension, $2a/W$. The R-curve thus obtained is found to be independent of the initial crack length. Broek [1966] carried out tensile tests on center cracked panels of 2024-T3 and 7075-T6 aluminum alloys and came up with results that supported the Krafft's hypothesis. He concluded that for a 2 to 1 change in initial crack length, the R-curve remained the same, which implied that it is independent of the initial crack length.

At this juncture, the validity of Krafft's hypothesis was accepted and efforts began to determine the R-curve for various materials. Freed, et al., [1971] carried out a series of experiments to find out the influence of specimen dimensions in the determination of fracture toughness values. They concluded that for the plane stress fracture toughness tests, valid K_c values can be obtained if the specimen configuration is such that the range $0.15 \leq 2a/W \leq 0.5$ is maintained.

Boyle [1962] found out that the effective crack length could be obtained directly using the compliance technique based on crack opening displacement (COD) measurements (thereby eliminating the need for plastic zone corrections). Later researches concentrated on evaluating Multiple-Site Damage (MSD) cracks on single member, joints and welded structures, and multiple load path (built-up structures) involving successive failure of multiple members.

3.0.2: Objectives

The primary objective of this effort was to determine the fracture strength for baseline (i.e., non-corroded) specimens of aluminum alloys 2024-T3 and 7075-T6 and to study the effects of corrosion damage on fracture strength in the same alloys. The study uses the R-curve approach for determining fracture strength of aluminum alloys.

The past researches were done on plain metal sheets and concluded that the R-curve is unique for a material when certain factors like temperature, strain rate (load rate) are maintained appropriately. The effect of initial crack length on R-curve is yet unclear though the Krafft's hypothesis is widely accepted. Aging aircraft loose material from prolonged exposure to corrosive environments. Hence it is necessary to have fracture toughness data on corroded panels to address the corrosion phenomenon in the initial design phase. Artificial corrosive environments provide a way to simulate the corrosive impacts on aluminum. Popular among such attempts are Exfoliation corrosion method and Salt spray chamber. Exfoliation principle is adopted in this research for its simple procedure and effective simulation of corrosive environments. The R-curve test conducted on these specimens provides a means to estimate the effects of varied thickness loss levels in relation with the baseline (non-corroded) specimens.

The study utilized the LEFM concepts to determine the R-curve since the plastic zone developed is in the order of material thickness and far less than the other parameters like crack-length and width. Both the compliance method and conventional plastic zone method were applied for determining the R-curve of the specimen.

3.1: Specimen Preparation

To reinforce the validity of the experimentally-determined R-curves, multiple replication testing was conducted; the test matrix for this effort is given in Table 3-1. The experimental treatments applied to the specimens were material specification (2024-T3, 7075-T6), specimen thickness (0.040, 0.063, 0.090 inches), and corrosion damage level (0%, 10%, 20%, 30% thickness loss). Each combination of parameters was replicated two times. The procedures used to prepare the specimens are outlined below.

3.1.1: Specimen Initial Preparation

Test specimens were 4 inches wide and 12 inches long (refer to Figure 2-1) and were cut

from the rolled sheets so the cracks would grow in the T-L direction. All specimens were degreased, dried and weighed to get their initial weight. Then the specimens were covered all over using 3M electroplating tape leaving only a 1 inch wide strip exposed in the middle of one side which was to be corroded.

3.1.2: Corrosion Procedure: Exfoliation Corrosion

As with the fatigue crack growth specimens in Section 2, the specimens used here were corroded in the ASTM EXCO solution [ast34] as outlined in Section 2.1. To reiterate, 234 grams of NaCl, 50 grams KNO_3 and 6.3 ml of HNO_3 were added to de-ionized water to make 1000 ml of solution. The initial pH of the solution was around 0.4 as confirmed by an electronic pH meter.

The specimens were kept immersed in the solution and allowed to corrode. The pH of the solution gradually increased as the corrosion progressed and reached approximately 3.0 when the corrosion solution had been exhausted. At this point, the specimens were taken out and a fresh solution was made for the next run. Before the start of the next run, the specimens were cleaned, checked for leakage through the tape (and re-taped if needed), dried and weighed for measuring the thickness loss. To determine the thickness loss incurred by the specimens, we used either the weight method that relies on the weight of the specimens before and after the corrosion process, Equation 2.1, or the direct measurement method using the point micrometer, Equation 2.2. The exposure times given in Section 2.1 were used to guide the immersion times for these specimens. Table 3-2 gives the thickness loss data for all of the corroded specimens used in the R-Curve determination. All of the data is based on the direct measurement of thickness loss method.

3.1.3: Specimen Final Preparation/Fabrication

The specimens were fabricated per the guidelines given by the ASTM E-561 [ast561].

They were notched in the center (see Figure 2.2) with a jeweler's saw to a length of approximately 0.50 inches and width of approximately 0.04 inches; the notch was required to make it easy to introduce fatigue cracks upon cyclic loading. Also the specimens were drilled and tapped on the specimen vertical centerline to hold the MTS model 632 clip-on strain gage which was used to measure the crack opening displacement during the loading..

3.2: Experimental Procedures

The R-curve testing, including specimen design, was conducted in accordance with ASTM E-561 [ASTM E 561]. The crack-length at the end of pre-cracking was the initial crack length for the R-Curve tests. The MTS Teststar II software was used to record the axial load, axial displacement, crack opening displacement (COD) using a clip gage, and time for the loading intervals. The crack lengths were measured using the traveling microscope during successive load intervals.

3.2.1: Plastic Zone Correction Method

From the data recorded, we computed the physical crack-length and then applied the plastic zone correction to get the effective crack-length as a function of K. Two steps of iteration were sometimes necessary to arrive at the correct effective crack-length. The crack resistance K_r was calculated using the relation,

$$K_r = \left(P/_{WB}\right)\sqrt{a}\left[1.77 - 0.177\left(2a/_{W}\right) + 1.77\left(2a/_{W}\right)^2\right] \quad (3.1)$$

where a is the effective crack-length. The R-curve was plotted with the resistance values in the y-coordinates and the crack growth increment in the x-coordinates (relative to the end of pre-cracking crack length).

3.2.2: Compliance Measurement Method

This method uses the inverse slope of the load versus crack opening displacement relationship; this inverse slope, $2v/P$, is also called the compliance factor. The compliance curve is a plot of the compliance factor versus $2a/W$, which after calibration may be used to get the effective crack length directly using the COD values. The compliance curve can be developed by taking several specimens of various initial crack-lengths, recording the initial slope of each specimen under elastic loading and plotting the reciprocal slopes (after normalizing the reciprocal slopes obtained for material thickness and elastic modulus) against the crack-length to specimen width ratio. The compliance curve can also be developed from a curve fit equation derived experimentally for the center cracked tensile specimens.

The compliance curve developed may consist of error that needs to be calibrated for each specimen. First the initial slope of the load-displacement from the respective test record is calculated which corresponds to the starting crack-length of the specimen. From this initial slope value, the reciprocal slope is calculated and then normalized to get a compliance value corresponding to the starting crack-length. This compliance value is entered into the compliance curve and the respective crack-length is computed. The crack-length thus computed is called the predicted initial crack-length.

If the actual initial crack-length and the predicted crack-length differ by more than 0.003W, the compliance curve is calibrated to adjust with the actual crack-length. Then the calibrated compliance curve can be used with the load-displacement record to get the effective crack-length at various values of the normalized ratios of displacement to load. The crack resistance values are computed using the effective crack-length obtained above. Finally, the R-Curve is plotted using the crack resistance and the increments of crack-length, similar to the plastic zone correction method.

In our experience, the plastic zone correction method was much easier to use than the compliance method. We had an advantage in using the plastic zone method in that we had

directly measured crack lengths from the traveling microscope. With difficulties in establishing its initial slope and subsequent sensitivity to the value of the slope, the compliance method was judged to be unsatisfactory in this application.

3.3: Experimental Results

From the experiments conducted and the data recorded, the R-curves for alloys 2024-T3 and 7075-T6 specimens are determined for various thickness loss levels. In our experience, the R-curves determined using the plastic zone method proved to be more accurate and reliable than those obtained using the compliance method. The crack growth resistance value K_r at the instability point is regarded as K_c, the fracture toughness of that specimen.

The fracture toughness of 2024-T3 baseline specimens with thickness 0.063" is found to be 49.25 ksi-√in and that of 0.040" to be 49.54 ksi-√in. The fracture toughness of 7075-T6 specimens is computed to be 59.9 ksi-√in for 0.063" thick specimens and 62.8 ksi-√in for 0.090" thick specimens. The tabulated values for different levels of thickness loss for the specimens are as given in Table 3-3.

The plots showing R-curve for baseline and corroded specimens are given in Figures 3-2 through 3-5. The plots indicate the differences in the R-curves for the baseline and corroded specimens. From these Figures, it is difficult to quantify the differences in critical fracture toughness, K_C, but Table 3-3 provides the data. We can see from the Table that there is a substantial reduction in K_C for all materials and nominal thicknesses as the level of corrosion damage is increased through 30% thickness loss.

As in the case of the crack growth data in Section 2, we were interested in the possibility of a clear relationship between the observed reduction in K_C and thickness loss. Because of a much smaller data set in this case, a statistical comparison was not feasible. However, we can make an observation based on the data in hand. In the case of 2024-T3, the 0.063 inch nominal plate is reduced to approximately 0.044 inches when damaged to 30% thickness loss.

Comparing the K_C values for 0.063/30% and 0.040/0%, we see that the corrosion-damaged specimen has a much smaller fracture toughness (30.7 ksi-√in.) than the baseline specimen of approximately the same thickness (49.5 ksi-√in.). This result is borne out again considering the case of 0.090/30% vs. 0.063/0% (which have approximately the same thickness). Again the corroded specimen has a lower fracture toughness (36.8 ksi-√in.) than the baseline specimen (59.9 ksi-√in.). Thus, it seems that in the case of fracture toughness (unlike in crack growth), a simple thickness correction will be insufficient to predict the reduction of toughness in a corrosion-damaged structure. Further study will be required to clarify this situation.

3.4: Concluding Remarks - Fracture Toughness

The R-curves for the materials used here show that the fracture toughness values decrease with increasing corrosion-induced thickness loss, thus confirming that corrosion is a phenomenon that has an impact on the fracture toughness of aluminum alloys. In contrast to the case of crack propagation, however, there currently seems to be no basis for scaling the toughness reduction directly with the thickness loss. The possibility exists that a scale factor exists that will bring the results into agreement, but that issue will have to be explored in subsequent efforts. Finally, our experience was that the plastic zone correction method of computing fracture toughness was much more accurate when compared to the compliance method. Difficulty in establishing the initial value of the force/deflection slope was the primary factor in rejecting that method.

4.0: Concluding Remarks

The overarching theme of this effort was to obtain material response data that could illuminate the effect corrosion has on the structural integrity of representative aircraft aluminum alloys. Specifically, we studied alloys 2024-T3 and 7075-T6, both of which are common in the older elements of the USAF inventory, e.g., the KC-135. Two aspects of structural integrity were explored: fatigue crack growth rate and fracture toughness. In both cases, we found that there was a clear degradation of the material performance when specimens had been damaged by corrosion. The crack growth rate increased at increasing damage levels (defined as percent thickness loss) and the fracture toughness decreased as the damage increased. Both of these results are intuitively correct, but until now, had not been clearly explored.

The increased crack growth rate was found to scale linearly with thickness loss and thus could be completely described by the reduced cross sectional area and resulting increased stress. Statistical hypothesis testing showed this to be so. On the other hand, the decrease in fracture toughness did not scale linearly with thickness loss. This aspect of the results needs more investigation to define the relationship between thickness loss and decreased toughness.

Figure 1-1 shows the relationship between crack growth rate, fracture toughness and inspection intervals for USAF aircraft. The data provided in this report is now available for maintenance planners to use in adjusting inspections to account for the possibility of hidden corrosion damage in their airframes. Also, these data could be used in computational models of airframe structural integrity.

5.0: References

ASTM E 561, 1986, *Standard Practice for R-Curve Determination*, American Society for Testing and Materials.

ASTM E 647, 1993, *Test Method for Measurement of Fatigue Crack Growth Rates*, American Society for Testing and Materials.

ASTM G 34, 1984, *Standard Test Method for Exfoliation Corrosion Susceptibility in 2XXX and 7XXX Series Aluminum Alloys (EXCO Test)*, American Society for Testing and Materials.

Atluri, S.N. and P. Tong, 1991, "Computational Schemes for Integrity Analyses of Fuselage Panels in Aging Airplanes," in *Structural Integrity of Aging Airplanes*, S.N. Atluri, S.G. Sampath and P. Tong, eds., Springer-Verlag, 15-35.

Baldwin, J.D., 1995, *The Effect of Corrosion on Fatigue Crack Growth Rates in Aircraft Structural Aluminum Alloys*, Final Report, AFOSR SFRP.

Baldwin, J.D.,1996, *Statistical Analysis of Fatigue Crack Growth Rate Data for 7075-T6 Aluminum Damaged by Prior Corrosion*, Final Report, AFOSR SFRP.

J.D. Baldwin, T.B. Mills and C.A. Paul, 1997, "Statistical Analysis of Fatigue Behavior of Aluminum Alloys in the Presence of Prior Corrosion," *Fatigue of New and Ageing Aircraft*, 19th ICAF Symposium, 1063-1074.

Beuth, J.L. and J.W. Hutchinson, 1994, "Fracture Analysis of Multi-Site Cracking in Fuselage Lap Joints," *Computational Mechanics*, 13, 315-331.

Blackburn, W.S., W.S. Hall and D.P. Rooke, 1995, "Boundary Element Analysis of Crack Intersection, Initiation and Growth at Pin Loaded Holes," *Fatigue and Fracture of Engineering Materials and Structures*, 18 (9), 949-957.

Boyle, R. W., 1962, *Materials Research and Standards*, Vol. 2, 646-651.

Broek, D., 1966, *The Residual Strength of Aluminum Alloy Sheet Specimens Containing Fatigue Cracks or Saw Cuts*, NLR-TR M2143, National Space Laboratory, Amsterdam.

Broek, D., 1993, *The Effects of Multi-Site-Damage on the Arrest Capability of Aircraft Fuselage Structures*, TR 9302, FractuREsearch Corp.

Campbell, G.S. and R. Lahey, 1984, "A Survey of Serious Aircraft Accidents Involving Fatigue Fracture," *International Journal of Fatigue*, 6(1), 25-30.

Chang, J.C.I., 1995, "Aging Aircraft Science and Technology Issues and Challenge and USAF Aging Aircraft Program," *Structural Integrity in Aging Aircraft*, AD-Vol. 47, American Society of Mechanical Engineers, 1-7.

Chaudhuri, J., Y.M. Tan, V. Gondhalekar and K.M. Patni, 1994, "Comparison of Corrosion-Fatigue Properties of Precorroded 6013 Bare and 2024 Bare Aluminum Alloy Sheet Materials," *Journal of Materials Engineering and Performance*, 3(3), 371-377.

Chubb, J.P., T.A. Morad, B.S. Hockenhull and J.W. Bristow, 1991a, "The Effect of Exfoliation Corrosion on the Fatigue Behavior of Structural Aluminum Alloys," *Structural Integrity of Aging Airplanes*, Atluri, Sampath and Tong, eds., 87-97.

Chubb, J.P., 1991b, "Effect of Environment and Corrosion on the Fatigue of Structural Aluminum Alloys," *Aluminum Today*, September 1991, 44-49.

Chubb, J.P., T.A. Morad, B.S. Hockenhull and J.W. Bristow, 1995, "The Effect of Exfoliation Corrosion on the Fracture and Fatigue Behavior of 7075-T6 Aluminum," *International Journal of Fatigue*, 17(1), 49-54.

Doerfler, M.T., A.F. Grandt, R.J. Bucci and M. Kulak, 1994, "A Fracture Mechanics Based Approach for Quantifying Corrosion Damage," *Proceedings of the Tri-Service Conference on Corrosion*, Orlando Florida, 433-444.

Du, M.L., F.P. Chiang, S.V. Kagwade and C.R. Clayton, 1995, "Effect of Corrosion on the Subsequent Fatigue Properties of Aluminum Alloy Sheet," *Proceedings of the 1995 SEM Spring Conference on Experimental Mechanics*, June 12-14, Grand Rapids, MI, 133-138.

Freed, C. N. and A.M. Sullivan, 1971, *The Influence of Geometric Variables on K_C Values for Two Thin Sheet Aluminum Alloys*, NRL Report 7270, Naval Research Laboratory.

Gangloff, R.P., 1990, *Corrosion Fatigue Crack Propagation in Metals*, NASA CR 4301, Washington, D.C.: National Aeronautics and Space Administration.

Gangloff, R.P., R.S. Piascik, D.L. Dicus and J.C. Newman, 1994, "Fatigue Crack Propagation in Aerospace Aluminum Alloys," *Journal of Aircraft*, 31(3), 720-729.

Harmsworth, C.L., 1961, *Effect of Corrosion on the Fatigue Behavior of 2024-T4 Aluminum Alloy*, ASD Technical Report 61-121, Aeronautical Systems Division, Wright-Patterson AFB.

Harris, C.E., J.H. Starnes, Jr. and J.C. Newman, Jr., 1995, "Development of Advanced Structural Analysis Methodologies for Predicting Widespread Fatigue Damage in Aircraft Structures," in *Proceedings of the FAA-NASA Sixth International Conference on the Continued Airworthiness of Aircraft Structures*, C.A. Bigelow, ed., 139-164.

Hendricks, W.R., 1991, "The Aloha Airlines Accident - A New Era for Aging Aircraft,", *Structural Integrity of Aging Airplanes*, Atluri, Sampath and Tong, eds., 153-165.

Hoeppner, D.W., L. Grimes, A. Hoeppner, J. Ledesma, T. Mills and A. Shah, 1995, "Corrosion and Fretting as Critical Aviation Safety Issues: Case Studies, Facts and Figures from U.S. Aircraft Accidents and Incidents," *International Committee on Aeronautical Fatigue*, 22 pages.

Irwin, G. R. and J.A. Kies, 1954, "Critical Energy Rate Analysis of Fracture Strength", *Welding Research Supplement*, Vol. 33, 193s-198s.

Jeong, D.Y. and J.C. Brewer, 1995, "On the Linkup of Multiple Cracks," *Engineering Fracture Mechanics*, 51 (2), 233-238.

Kemp, R.M.J., R.N. Wilson and P.J. Gregson, 1993, "A Comparison of the Corrosion Fatigue Properties of Plate Aluminum Alloys for Aerospace Applications," *Journal of Aerospace Engineering*, Vol. 207, 97-104.

Krafft, J. M., A.M. Sullivan, and R.W. Boyle,1961, *Proceedings, Crack Propagation Symposium*, College of Aeronautics, Vol. 1, Cranfield, England, 8-26.

Leybold, H.A., H.F. Hardrath and R.L. Moore, 1958, "An Investigation of the Effects of Atmospheric Corrosion on the Fatigue Life of Aluminum Alloys," NACA TN-4331.

Lincoln, J.W., 1995 "The USAF Approach to Attaining Structural Integrity of Aging Aircraft", *Structural Integrity in Aging Aircraft,* C.I. Chang and C.T. Sun, Eds., ASME, Vol. 47, pp. 9-19.

Luzar, J., 1995, *Integrated C/KC-135 Corrosion Program Round Robin Testing: Pre-Corroded Fatigue Crack Growth Rate Test Plan*, Boeing Defense & Space Group, Product Support Division, Wichita KS.

Mills, T.B. and D.W. Hoeppner, 1995, "The Effects of Exfoliation Corrosion on the Fatigue Response of 7075-T651 Aluminum Plate," Quality and Integrity Design Center, Department of Mechanical Engineering, University of Utah.

Molent, L. and R. Jones, 1993, "Crack Growth and Repair of Multi-Site Damage of Fuselage Lap Joints," *Engineering Fracture Mechanics*, 44 (4), 627-637.

Paris P., M. Gomez, and W. Anderson, 1961, "A Rational Analytic Theory of Fatigue", *The Trend in Engineering*, 13:9-14.

Park, J.H., T. Ogiso and S.N. Atluri, 1992, "Analysis of Cracks in Aging Aircraft Structures, With and Without Composite-Patch Repairs," *Computational Mechanics*, 10, 169-201.

Person, N.L., 1975, "Fatigue Properties of Prior-Corroded Aluminum Sheet Alloys," *Materials Performance*, December 1975, 22-26.

Pyo, C.R., H. Okada, L. Wang, F.W. Brust and S.N. Atluri, 1995, "Residual Strength Prediction for Aircraft Panels with Multiple Site Damage (MSD) Using the Elastic Plastic Finite Alternating Method (EPFEAM)," in *Structural Integrity of Aging Aircraft*, C.I. Chang and C.T. Sun, eds., ASME, 73-80.

Rankin, C.C., F.A. Brogan and E. Riks, 1993, "Some Computational Tools for the Analysis of Through Cracks in Stiffened Fuselage Shells," *Computational Mechanics*, 13, 143-156.

Samavedam, G. and D. Hoadley, 1994, *Fracture and Fatigue Strength Evaluation of Multiple Site Damaged Aircraft Fuselages - Curved Panel Testing and Analysis*, Final Report, DOT/FAA/CT-94/10, DOT-VNTSC-FAA-93-8.

Scheuring, J.N. and A.F. Grandt, 1994, "An Evaluation of Fatigue Properties of Aging Aircraft Materials," USAF Structural Integrity Program Conference, San Antonio TX.

Scheuring, J.N. and A.F. Grandt, 1995, "An Evaluation of Aging Aircraft Material Properties," *Structural Integrity of Aging Aircraft*, AD-Vol. 47, American Society of Mechanical Engineers, 99-110.

Schutz, W., 1995, "Corrosion Fatigue - The Forgotten Factor in Assessing Durability," 15th Plantema Memorial Lecture, 18th Symposium of the International Committee on Aeronautical Fatigue.

Singh, R., J.H. Park and S.N. Atluri, 1994, "Growth of Multiple Cracks and Their Linkup in a Fuselage Lap Joint," *AIAA Journal*, 32 (11), 2260-2268.

Tong, P., R. Greif and L. Chen, 1994, "Residual Strength of Aircraft Panels with Multiple Site Damage," *Computational Mechanics*, 13, 285-294.

Tong, P., 1994, "Influence of Fastener Holes on Residual Strength," *International Journal of Fracture*, 67, 315-324.

Vu, T.Q., 1999, *The Impact of Corrosion on Fatigue Crack Propagation in 7075-T6 Aluminum Alloy*, Master of Science Thesis, University of Oklahoma.

6.0: Figures

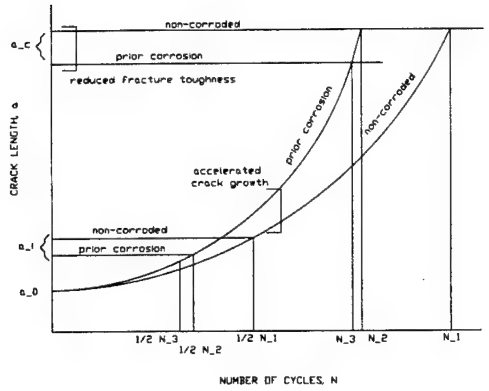

Figure 1-1: Relationship Between Corrosion Damage and Inspection Interval

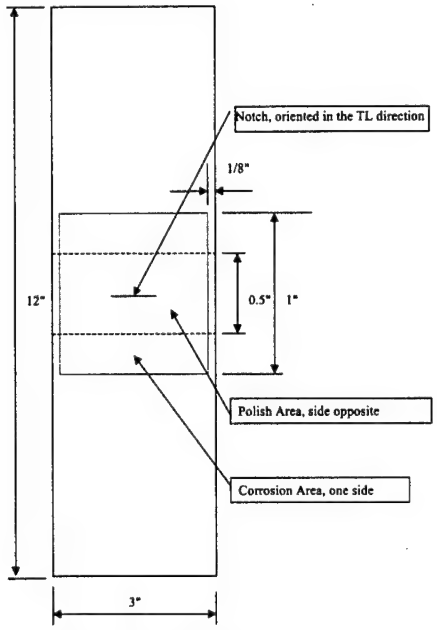

Figure 2-1: Middle Tension Test Specimen

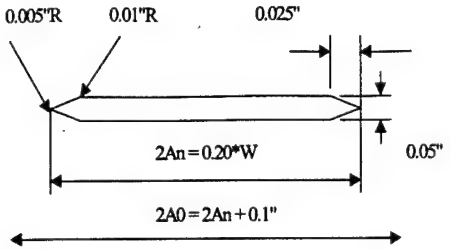

Figure 2-2: Starter Notch Geometry

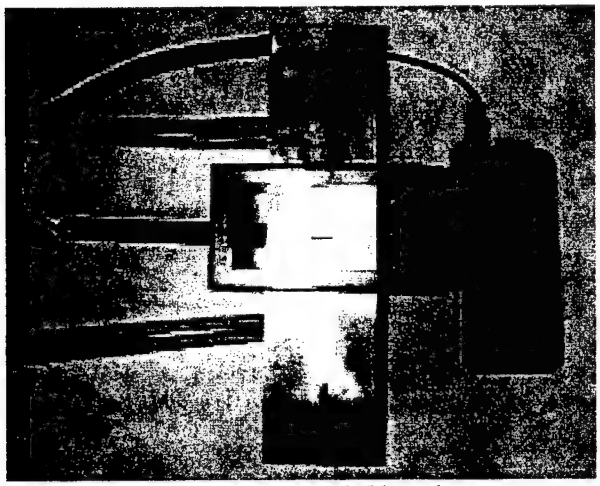

Figure 2-3: Environmental Chamber on Specimen

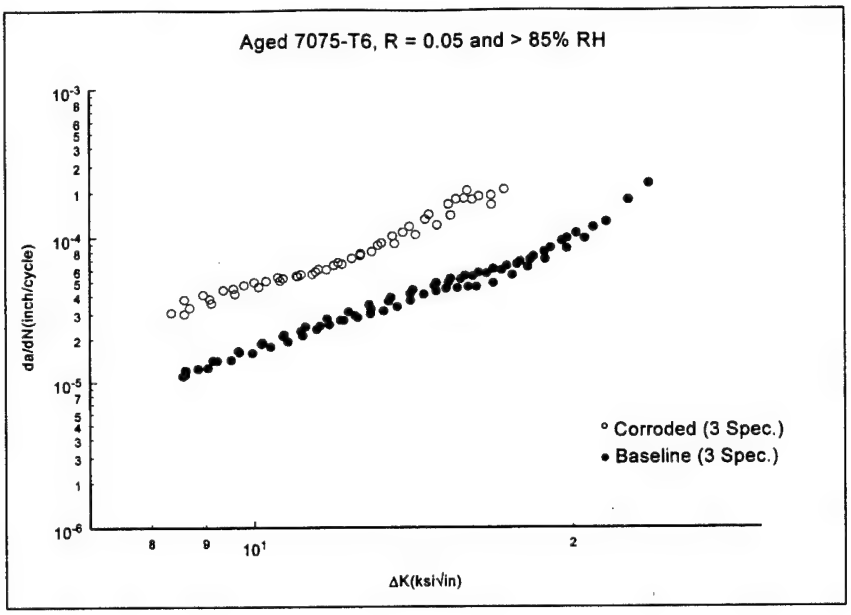

Figure 2-4: Fatigue Crack Growth Rate, Aged 7075-T6, No Thickness Correction

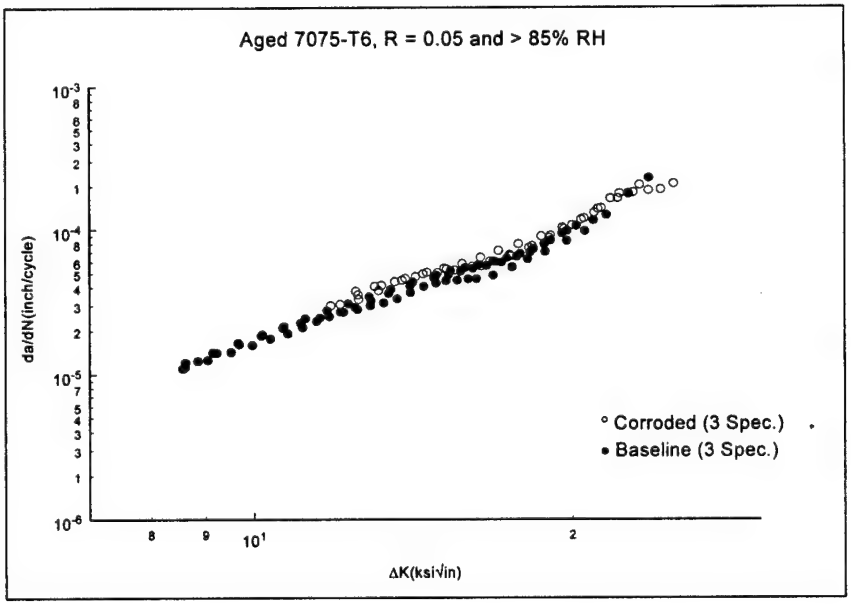

Figure 2-5: Fatigue Crack Growth Rate, Aged 7075-T6, Thickness Corrected

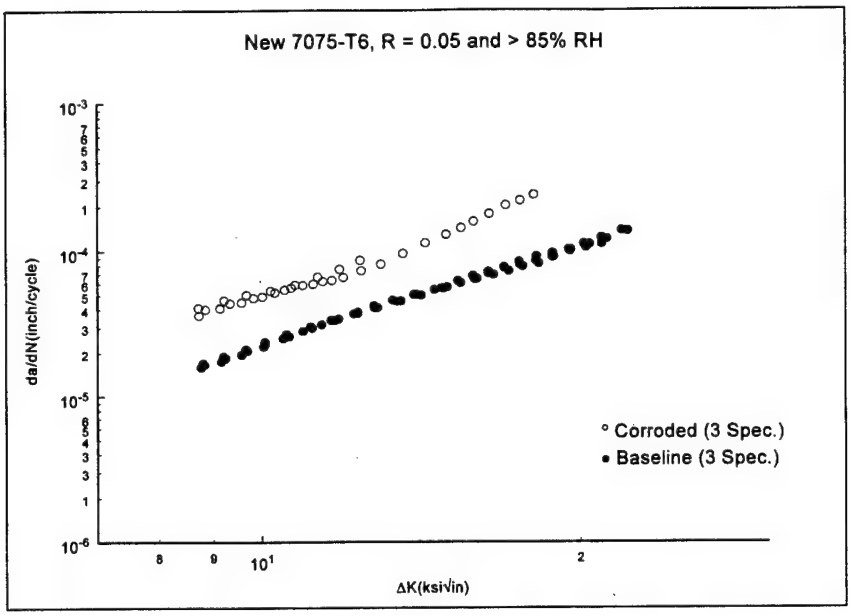

Figure 2-6: Fatigue Crack Growth Rate, New 7075-T6, No thickness Correction

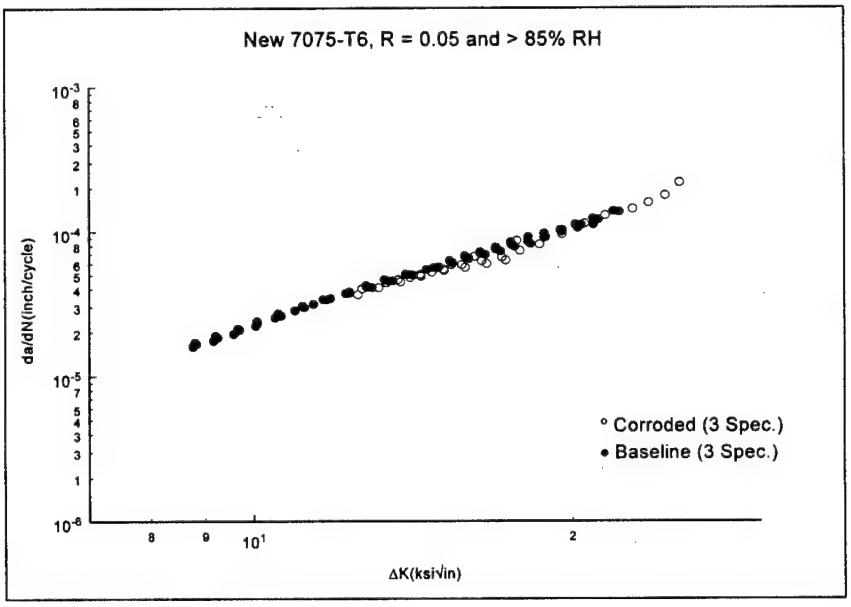

Figure 2-7: Fatigue Crack Growth Rate, New 7075-T6, Thickness Corrected

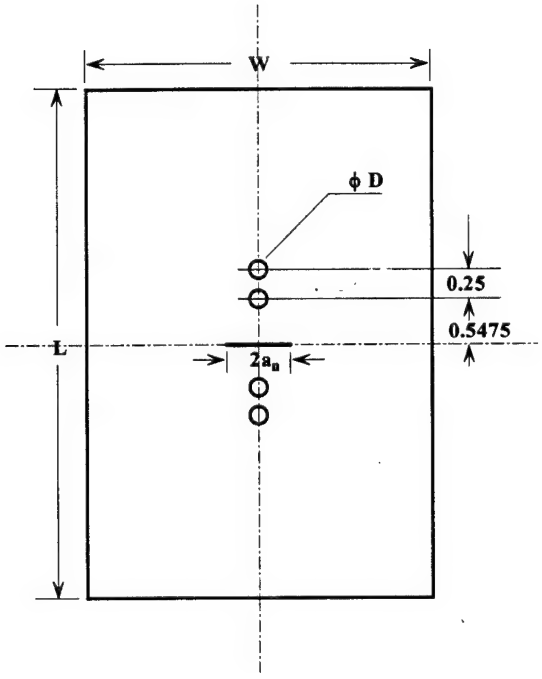

Figure 3-1: R-Curve Specimen Details, L = 12 inch, W = 4 inch

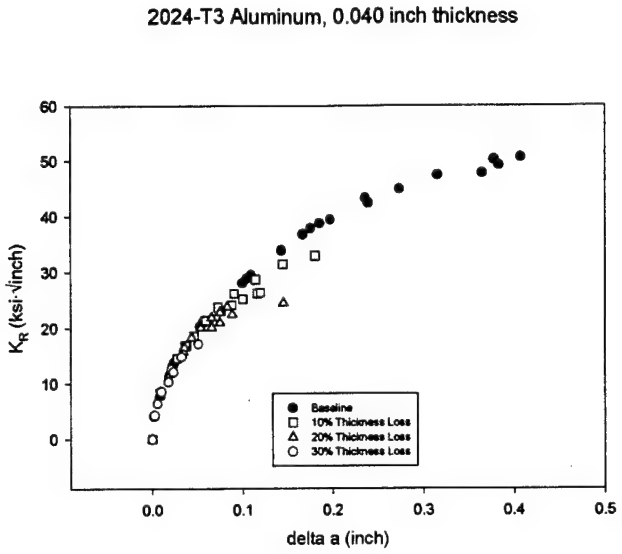

Figure 3-2: R-Curves vs. Thickness Loss for 2024-T3, 0.040 inch Thick Aluminum Sheet

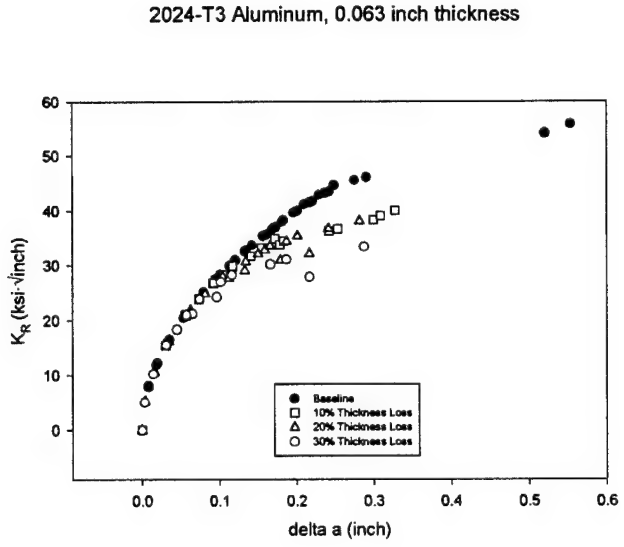

Figure 3-3: R-Curves vs. Thickness Loss for 2024-T3, 0.063 inch Thick Aluminum Sheet

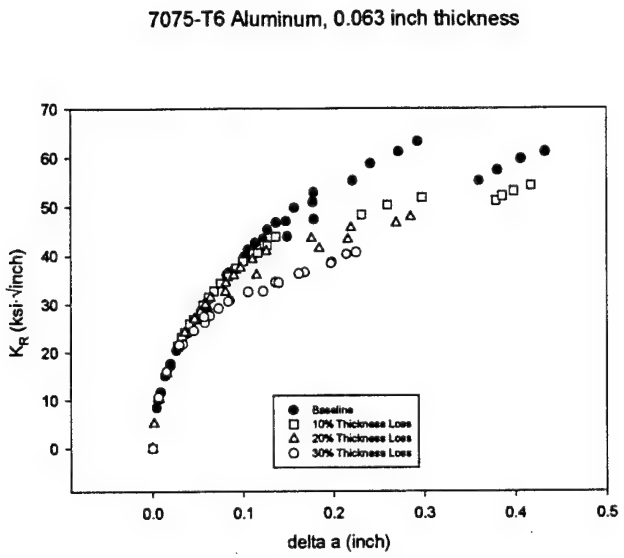

Figure 3-4: R-Curves vs. Thickness Loss for 7075-T6, 0.063 inch Thick Aluminum Sheet

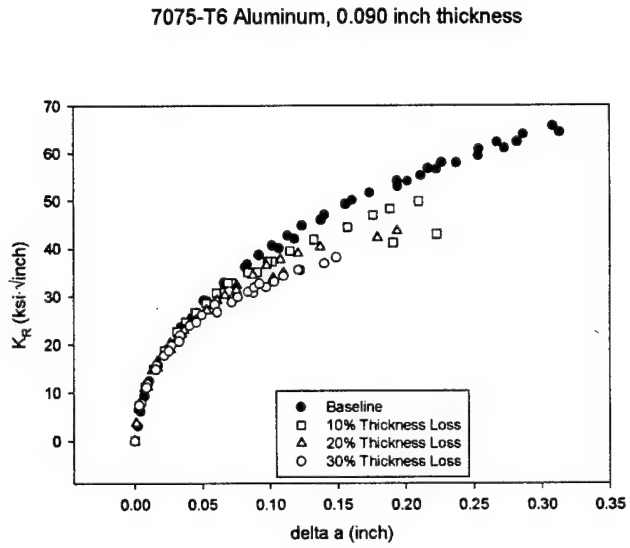

Figure 3-5: R-Curves vs. Thickness Loss for 7075-T6, 0.090 inch Thick Aluminum Sheet

7.0: Tables

	Percent Thickness Loss (192 Hours Immersion in EXCO sol'n)		
Specimen No.	Weight Loss	Micrometer	Microscope
1	31.5	29.1	
2	32.0	30.7	
3	33.5	31.2	31.6
4	29.1	30.8	
5	26.7	27.3	
6	30.9	31.2	30.8
7	32.6	30.6	
8	25.1	25.1	
9	26.1	23.6	23.4
10	25.8	25.7	
11	28.2	27.4	26.2
12	30.5	27.8	

Table 2-1: Percentage Thickness Loss in Aged 7075-T6 Material Specimens

Specimen No.	Percent Thickness Loss (192 Hours Immersion in EXCO sol'n) Weight Loss	Micrometer	Microscope
1	30.0	29.7	
2	27.1	27.4	
3	28.1	29.6	30.6
4	30.6	30.2	
5	28.1	28.7	
6	29.7	29.3	29.9
7	28.9	30.5	
8	30.2	30.2	29.3
9	32.3	32.7	
10	31.6	32.7	
11	27.9	27.7	26.4
12	28.0	28.7	

Table 2-2: Percentage Thickness Loss in New 7075-T6 Material Specimens

	Number of Test Replications							
	Baseline				Corroded			
	R = 0.05		R 0.50		R = 0.05		R = 0.50	
Mat'l	< 15% RH	> 85% RH	< 15% RH	> 85% RH	< 15% RH	> 85% RH	< 15% RH	> 85% RH
Aged	3	3	3	3	3	3	3	3
New	3	3	3	3	3	3	3	3

Table 2-3: Crack Growth Test Matrix

Stress Ratio	Aged Material				New Material			
	R = 0.05		R = 0.50		R = 0.05		R = 0.50	
RH	< 15%	> 85%	< 15%	> 85%	< 15%	> 85%	< 15%	> 85%
ΔK = 9, UC				SD	SD	SD		SD
ΔK = 9, TC								
ΔK = 10, UC			SD	FAIL	SD	SD	SD	SD
ΔK = 10, TC								
ΔK = 11, UC			SD	SD	SD	SD	SD	SD
ΔK = 11, TC			ISD			ISD		
ΔK = 12, UC	SD	SD		SD	SD	SD		
ΔK = 12, TC	ISD	ISD	ISD	ISD	ISD	ISD	ISD	ISD
ΔK = 13, UC	SD	SD				SD		
ΔK = 13, TC	ISD	SD(*)	ISD	ISD	ISD	ISD	ISD	ISD
ΔK = 14, UC	SD	SD						
ΔK = 14, TC	ISD	ISD		ISD	ISD	SD(*)	ISD	ISD
ΔK = 15, UC	SD	SD						
ΔK = 15, TC	ISD	ISD			ISD	SD(*)		ISD
ΔK = 16, UC	SD	FAIL						
ΔK = 16, TC	ISD	ISD			ISD	ISD		
ΔK = 17, TC	FAIL	SD						
ΔK = 17, TC	ISD	ISD			ISD	ISD		

UC = No thickness correction
TC = Thickness correction
SD = Statistically significant difference in *da/dN*
ISD = Statistically insignificant difference in *da/dN*
FAIL= To fails either Normality test, Equal Variance test or both.

Table 2-4: Results of Statistical Analysis

Material	Thickness (inch)	% Thickness Loss	Number of Test Replications
2024-T3	0.040	0	3
		10	2
		20	2
		30	2
	0.063	0	3
		10	2
		20	2
		30	2
7075-T6	0.063	0	3
		10	2
		20	2
		30	2
	0.09	0	3
		10	2
		20	2
		30	2

Table 3-1: R-Curve Test Matrix

Material	Specimen No.	Original Thickness, inch	Final Thickness, inch (Direct Measurement)	% Thickness Loss	Nominal % Thickness Loss
2024-T3	C_1	0.04	0.0318	20.50	20
	C_5		0.0323	19.25	20
	S_5	0.063	0.0558	11.43	10
	S_6		0.0555	11.90	10
	S_M		0.0508	19.37	20
	B_2		0.0496	21.27	20
	S_A		0.0448	28.89	30
	S_1		0.0458	27.30	30
7075-T6	A_1	0.063	0.0556	11.75	10
	A_12		0.055	12.70	10
	A_9		0.0493	21.75	20
	A_6		0.0508	19.37	20
	A_4		0.0485	23.02	30
	A_5		0.0478	24.13	30
	D_1	0.09	0.0808	10.22	10
	D_3		0.0815	9.44	10
	D_4		0.0737	18.11	20
	D_9		0.0712	20.89	20
	D_6		0.0638	29.11	30
	D_7		0.0632	29.78	30

Table 3-2: Thickness Reduction Data for R-Curve Specimens

Material Type	Nominal Thickness (B_{nom})	Nominal Thickness Loss (%)	Actual Thickness (B_{act})	Fracture Toughness K_c (Average)
2024-T3	0.040	0	0.040	49.5
		10	0.036	29.6
		20	0.032	21.8
		30	0.028	12.1
	0.063	0	0.063	49.2
		10	0.057	38.3
		20	0.050	35.1
		30	0.044	30.7
7075-T6	0.063	0	0.063	59.9
		10	0.57	53.1
		20	0.50	46.7
		30	0.44	40.4
	0.090	0	0.090	62.8
		10	0.081	46.4
		20	0.072	39.2
		30	0.063	36.8

Table 3-3: Critical Fracture Toughness Values for Varying Thickness Loss Values